IEEE Access
Multidisciplinary | Rapid Review | Open Access Journal

Received May 23, 2021, accepted May 28, 2021, date of publication June 3, 2021, date of current version June 10, 2021.

Digital Object Identifier 10.1109/ACCESS.2021.3085695

Application of Numerical Simulation for Metallized Film Capacitors Electrodes Design

VICTOR O. BELKO, (Member, IEEE), OLEG A. EMELYANOV, (Senior Member, IEEE), IVAN O. IVANOV, (Member, IEEE), ANDREY P. PLOTNIKOV, (Member, IEEE), AND EFREM G. FEKLISTOV, (Graduate Student Member, IEEE)

Peter the Great St. Petersburg Polytechnic University, 195251 Saint Petersburg, Russia

Corresponding author: Victor O. Belko (vobelko@spbstu.ru)

This work was supported by the Russian Science Foundation under Project 19-79-10075.

ABSTRACT Polymer film capacitors are widely used in modern power equipment, because of excellent volumetric characteristics in combination with high-voltage application ability. Using segmented electrodes of nanometer thickness increased the capacitor's performance and reliability because of the self-healing feature. In this paper, we present the results of the experimental investigation and numerical simulation of electrothermal destruction of the metallized film capacitors segmented electrodes during the self-healing process. The destruction processes were investigated for both a single gate and single segment, comprising four parallel gates connected to the segment. The numerical simulation was conducted by means of COMSOL Multiphysics software. The model takes into account the heat flow from metal layer to polymer film since it has significant influence on the destruction process. Based on a good agreement of experimental and numerical results, the simulation model was proposed for the real metallized film capacitor segmented electrodes design. The model allows evaluating the single segment isolating time during self-healing, the energy required for the isolating, effective value of segmented electrodes surface resistance.

INDEX TERMS Capacitors, plastic films, metallization, electrothermal effects, numerical simulation.

I. INTRODUCTION

The miniaturization of electronic passive components and their operation in harsh environmental conditions are growing trends in the modern industry. The miniaturization leads to space and weight saving that is crucial in areas, such as automotive, aerospace, military power systems, and energy storage. Considering a harsh environment, it is important to note that the advances in wide bandgap semiconductor devices (e.g., SiC and GaN) have created new opportunities for energy efficient power conversion circuits operating at high temperatures [1], [2]. The most expensive passive component is usually a capacitor. Depending on the dielectric material, there are three main types of capacitors used in the above-mentioned areas: polymer film, ceramic, and electrolytic. Compared to the ceramic and electrolytic capacitors, metalized polymer film capacitors (MFC) are cost-effective, suitable for high voltage [3], and degrade by a ''graceful'' aging mechanism primarily caused by the self-healing ability.

The associate editor coordinating the review of this manuscript and approving it for publication was Norbert Herencsar.

The design of MFCs is well known. In the general case, MFC consists of two metallized polymer films, which are wound on a mandrel, forming a cylindrical capacitance element [3]. There are single- and multi-element capacitors. As a rule, high voltage/energy density capacitors consist of numerous capacitance elements that are connected in series and parallel for achieving the required voltage and capacitance. In this case cylindrical capacitance elements are usually flat-pressed for higher volumetric efficiency. Film chip-capacitors may be mentioned as an individual capacitor's type [4]. Different designs of MFCs are shown in Fig. 1.

The important parameter of any electric capacitor is a volumetric energy density, which is determined by the expression:

$$W_V = \frac{\varepsilon \varepsilon_0 E^2}{2} k, \tag{1}$$

where ε is a relative permittivity of dielectric material, $\varepsilon_0 = 8.85 \times 10^{-12}$ F/m is the dielectric constant, E is an electric field in the dielectric and k is a packaging factor. State-of-the-art MFCs have the value of W_V up to 2 J/cm^3 for long operation lifetime and up to 3 J/cm^3 for short one [5]–[7].

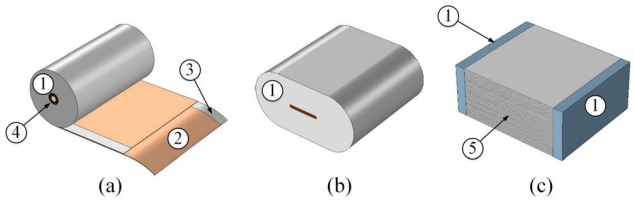

FIGURE 1. The view of cylindrical capacitance element (a), flat-pressed capacitance element (b) and film chip-capacitor (c): 1 – shoopage, 2 – metallization, 3 – non-metallized edge, 4 – mandrel, 5 – layers of metallized polymer film.

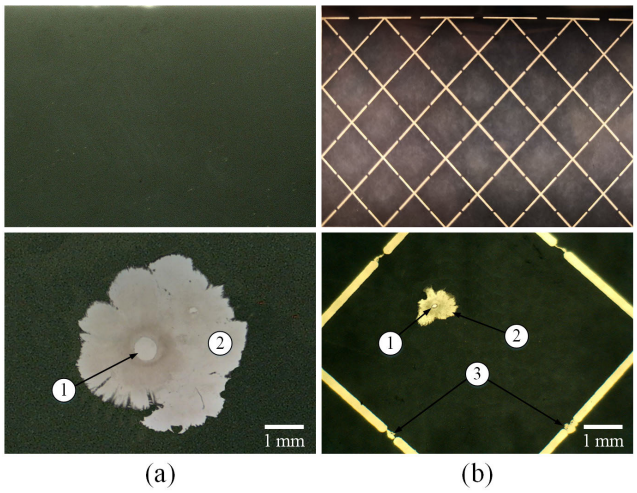

FIGURE 2. Photographs of all-over (a) and segmented (b) metallization after self-healing: 1 – breakdown channel, 2 – demetallized zone, 3 – destructed gates.

Currently, one of the most commonly used polymer capacitor films is the biaxially oriented polypropylene film (BOPP). Despite the low relative permittivity $\varepsilon = 2.2$, this film has the outstanding characteristics: high breakdown strength $E_{BD} =$ 600 – 700 kV/mm and very low loss tangent $\sim 10^{-4}$ [8]. The latter characteristic makes this material an ideal choice for pulsed power and power conditioning applications.

Nanometers thickness layers of metal evaporated on the polymer film surface are used as electrodes in MFCs. Usually, these electrodes are made of aluminum, zinc, or their combination. Metallized electrodes have higher resistance than foil electrodes, but provide the MFC with the unique feature – self-healing (SH). SH is an ability of MFC to restore its operating voltage after the dielectric breakdown. When the dielectric breakdown occurs, a small part of electrodes near the breakdown channel evaporates due to Joule heating caused by high current density (10^{11} – 10^{12} A/m^2) [9]. After isolating the breakdown channel, the capacitor restores its operating voltage. In MFCs with all-over electrodes, covering the whole surface of the polymer film, SH process lasts from units to tens of microseconds and is proportional to the capacitance. Single SH act does not lead to a significant capacitance decrease because the demetallization area is several units of square millimeters and even less [10], [11]. The example of SH act in all-over metallization is shown in Fig. 2a. However, numerous SH acts lead to a noticeable capacitance decrease and rise of the dielectric losses. Usually 5 – 10 % drop of the capacitance is used as a criterion of MFC's parametric failure [11], [12].

Nevertheless, the dielectric breakdowns in high voltage MFCs can quickly lead to a catastrophic failure. It is known that the energy dissipated in the breakdown place during SH (SH energy) is proportional to the capacitor's voltage – $W_{SH} \infty U^n$, where $n = 2.2 – 2.6$ [13]. High dissipated energy values lead to the intensive decomposition of the polymer dielectric and formation of the conducting carbon layer covering the demetallization area. Instead of isolated it becomes shunted by the carbon layer. This makes the SH ineffective. In order to limit the SH energy and to improve the reliability of high voltage MFCs the ultrathin electrodes or segmented electrodes can be used. Because of the thickness (3–5 nm) the ultrathin electrodes are characterized by a high value of the electrodes' resistance (100–300 Ω) and, consequently, capacitor's equivalent series resistance (ESR) and dissipation factor. That is why the segmented metallized electrodes are better solution for high current/voltage applications. In this type, the capacitor's electrodes are divided into segments interconnected by narrow gates (fuses). When the dielectric breakdown within the segment area occurs, the gates of the segment are electrothermally destructed. The defected segment with breakdown channel becomes isolated from the rest of the electrodes (Fig. 2b). Then the operating voltage of the capacitor restores [14].

The advantages of segmented electrodes:

- Lower SH energy value and shorter duration of SH process—because of a small size of the gate less energy is required for its destruction;
- Sources of heat dissipation are spaced apart–five low-energy sources for segmented versus one high-energy source for all-over metallization. This means less probability of the adjacent polymer layers heating and breakdown;
- Metallization surface resistance (10 – 30 Ω) is much lower than the resistance of ultrathin electrodes.

The disadvantages of segmented electrodes:

- Slightly lower capacitance for a given polymer film area because of inactive intersegment gap (up to 5 – 10 %);
- Faster capacitance degradation caused by SH acts—successful SH act means the whole segment cuts off from the active electrodes.

There are different patterns of segmented electrodes: T-patterns, mosaic (or diamond-like) patterns, etc. Traditionally, T-patterns have been used for high-voltage applications, but the MFCs with this type of pattern have higher capacitance degradation rate, because of the larger segment size. Mosaic patterns seem to be more universal but require individual design for different applications (DC, AC, high current, etc.). Segmented electrodes optimization allows increasing the performance and reliability of the MFCs,

TABLE 1. Parameters of investigated capacitor films.

Polymer film	Metallization metal	Film thickness	Metallization thickness	Surface resistance
PP	Zn	7 – 10 μm	10 – 20 nm	20 – 6 Ω
PP	Al	6 – 10 μm	7 – 20 nm	16 – 3 Ω

so they can operate at higher electric field for longer lifetime. The important stage in the design of new capacitors is the selection of polymer film, metal, and segmentation parameters: segments size, gates width, intersegment distance, and metallization thickness. Properly designed segmented electrodes are effective against breakdown currents, however remain functional during high ripple current operation. A model for numerical simulation of performance of developed segmentation designs could be a good way to reduce the time, cost, and risk associated with full-scale testing of MFCs under development.

In this paper we present the results of developing the model for simulation the behavior of segmented metallization during the MFC's operation. The simulation is based on the mathematical model considering the peculiarities of the destruction of thin metal layers evaporated on the polymer films. The simulation model is verified by the experiments on commercial capacitor segmented metallized films. There is a good agreement between the simulation and obtained experimental results.

II. MATERIALS AND METHODS

In the present paper two types of experiment investigations were conducted: small-scale and large-scale.

Experimental samples in both cases were prepared from commercial capacitor's polypropylene films with Zn or Al mosaic segmented metallization. Parameters of investigated polymer films are shown in Table 1. Both types of films had a segment's size 8 mm × 8 mm.

A. SMALL-SCALE EXPERIMENTS. SINGLE GATE DESTRUCTION

In the case of small-scale investigations, the aim was to study the regularities of electrothermal destruction of a single gate between two adjacent segments. Relatively simple experiments allowed us to check some assumptions for the developing model, and validate it for further scaling.

The experimental samples consisted of two segments connected by a narrow gate. The simplified scheme of the experimental set up with a test cell is presented in Fig. 3.

The main elements of the scheme are the generator of rectangular pulses, the experimental cell and low-inductive current probe. The potential and ground electrodes were placed on two neighboring segments. The voltage pulse of a rectangular shape and long duration (up to 200 μs) was

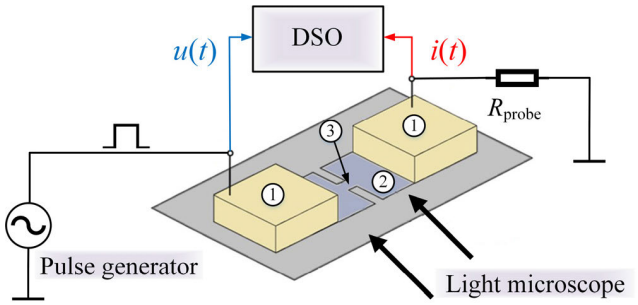

FIGURE 3. Scheme of experimental set up and test cell: 1 – electrodes, 2 – segments, 3 - gate.

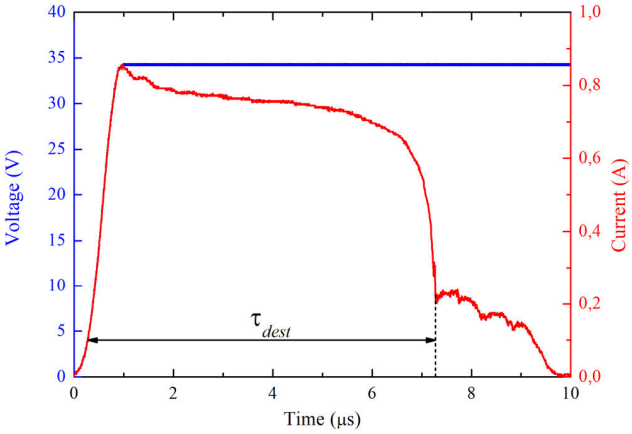

FIGURE 4. Typical waveforms of single gate destruction process.

applied to the cell. The pulse amplitude varied in 5 – 50 V range. The voltage drop across the experimental cell and the current flowing through the gate were measured by 2 GS/s digital storage oscilloscope. Typical waveforms of the process are presented in Fig. 4.

The moment of the sudden current drop corresponds to the destruction of the gate (τ_{dest}) and possible beginning of the second phase of SH process—microarc discharge. At a certain condition (low-middle voltage, high pressure, impregnation of the capacitor etc.), the microarc stage can be minimized or even eliminated. The absence of the microarc stage is a preferable way of SH process development since this minimizes the SH energy.

By the moment τ_{dest} the gate becomes traversed by a narrow demetallized crack. The propagation of this crack has an electrothermal nature.

To evaluate the energy input to the gate the specific action integral J is used:

$$J = \int_0^{\tau_{dest}} j(t)^2 \cdot dt, \tag{2}$$

where $j(t) = I(t)/A$ – current density in the gate, A – cross-section of the gate.

The specific action integral J was chosen as a measure of SH energy since it is more convenient for usage. Using of J

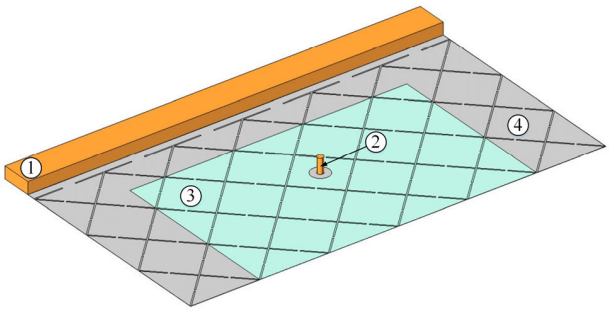

FIGURE 5. Experimental cell with the sample in large-scale investigations: 1 – potential electrode, 2 – ground electrode, 3 – upper polymer film, 4 – polymer film with segmented metallization.

allows us to get an accurate information about local energy dissipation, unlike the common characteristic

$$W = \int_0^{\tau_{dest}} U(t)I(t) \cdot dt, \tag{3}$$

comprising a portion of the energy dissipated in the gate and a portion of one dissipated in the rest part of metallized electrodes, contact resistance, etc.

B. LARGE-SCALE EXPERIMENTS. FOUR GATE DESTRUCTION, OR ONE SEGMENT ISOLATING

During the large-scale experiments, the simultaneous destruction of several gates connected to one segment was studied. This process imitates the real situation in the MFC during the breakdown and SH. In this case, the aim was the determination of the energy and time characteristics of the SH process.

In large-scale investigations, the experimental samples had a large number of segments. The electrical breakdown in one defected segment was simulated. The view of the experimental cell is shown in Fig. 5.

The potential electrode was placed on the heavy edge side of experimental sample and cylindrical ground electrode of a small diameter was placed on the center of a segment. An additional clear PP film (without metallization) was fixed on top of the experimental sample to simulate the confined interlayer space and heat transfer conditions as in the real MFC. The electrothermal destruction of the gates was also realized by applying rectangular voltage pulses of varying amplitude to the electrodes. The principle of the experimental set up remained the same as for the single gate scheme. The applied voltage varied in 50 – 300 V range. Varying durations of gate destruction processes were received by changing the amplitude of the voltage pulses.

For both small and large-scale experiments, the samples with the destructed gates were examined by means of light microscopy. The microphotographs of destructed area within the gate will be presented in the following section.

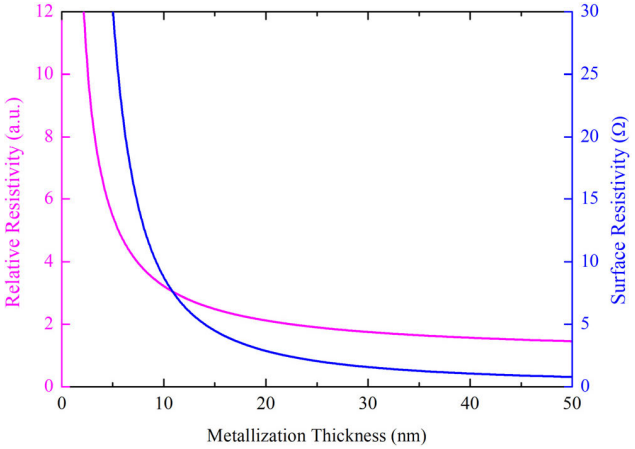

FIGURE 6. Dependence of resistivity and surface resistance of aluminum on its thickness, according to [15].

C. SIMULATION MODEL

The numerical model of electrothermal destruction was developed using COMSOL Multiphysics software. Electric Currents in Shells, Electrical circuit, Heat Transfer in Solids software modules with time dependent study were used. The model uses electric current and heat transfer equations:

$$\begin{aligned} \nabla j &= 0 \\ E &= -\nabla\varphi \\ j &= \sigma(T)E \end{aligned} \tag{4}$$

$$\rho(T)C(T) \cdot \frac{\partial T}{\partial t} = \lambda(T) \cdot \nabla^2 T + Q_V \tag{5}$$

where j is a current density, E is an electric field, φ is an electric potential, $\sigma(T)$, $\lambda(T)$, $\rho(T)$, $C(T)$ are material's electric conductivity, thermal conductivity, density and specific heat respectively, T is a temperature, Q_V is a volumetric power density. Temperature dependences of electrical and thermal material's parameters, the influence of metallization thickness on the value of electric conductivity (see the example for the aluminum in Fig. 6) and the latent heats of melting and evaporation are taken into account.

3D geometry of the model was important for calculating heat flows in all directions. As it was shown earlier [9], [16], the heat flow from the metallized electrodes to the polymer film is substantial even for the microsecond duration of the destruction processes.

As an example, the comparison of the shares of dissipated power density for heating the PP film and Al layer are presented in Fig. 7. Total power density 5.72×10^{15} W/m^3 is a result of 3×10^{11} A/m^2 current density in 20 nm thick Aluminum layer. For example, at this power rate it takes $\sim$ 13 μs to heat 20 nm of Al up to melting temperature $T_{melt} =$ 660 °C in the presence of polymer film. More than 90% of input energy is absorbed by polymer film. The presence of polymer significantly affects the dynamics of the gate destruction process. Moreover, for given current density the heat outflow (and consequently—the metallization heating

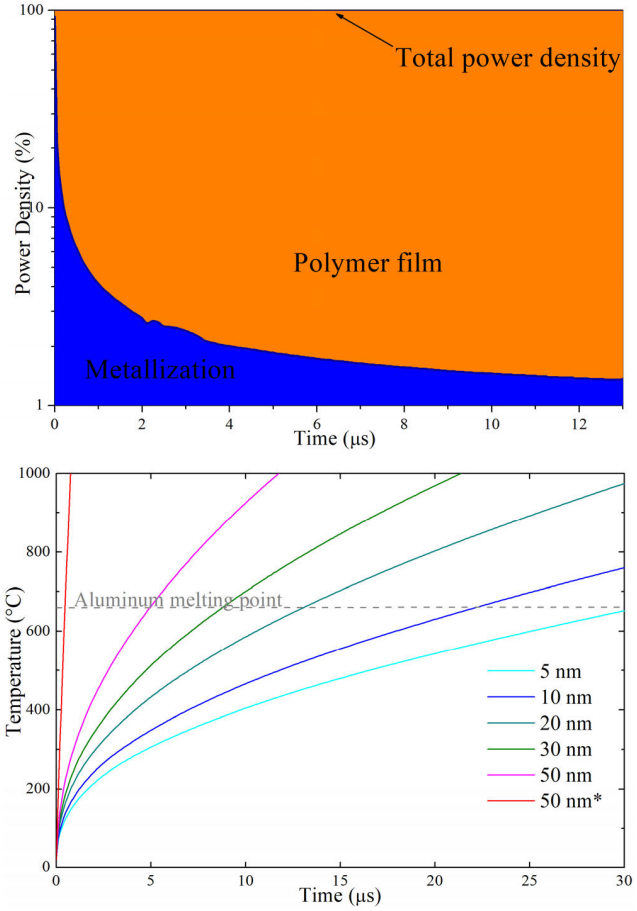

FIGURE 7. Upper: distribution of power densities in metallization–polymer film sandwich structure; bottom: heating rates for Al layers of different thicknesses at a given current density (50 nm* - without heat outflow).

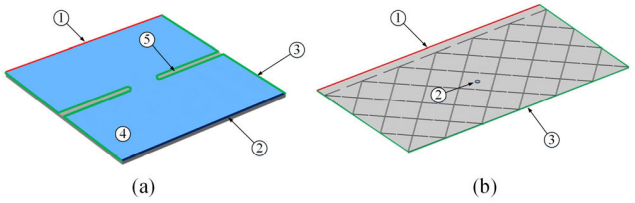

FIGURE 8. The calculation geometry and boundary conditions in small-scale (a) and large-scale (b) investigations: 1 – electric potential, 2 – ground, 3 – electric insulation, 4 – metallization, 5 – polymer film.

rate) strongly depends on the thickness of the metallization layer (see Fig. 7).

Geometric model and boundary conditions for small-scale and large-scale simulations are presented in Fig. 8.

The main assumption of the model is that there is fast heating, including consequent solid-liquid-vapor phase transition of metal layer caused by high current density. When the evaporation temperature T_{ev} is reached, there is a significant decrease in electric and thermal conductivities:

$$\sigma_{Me} = \begin{cases} \sigma(T), & T < T_{ev} \\ 1\ S/m, & T \geq T_{ev} \end{cases} \tag{6}$$

$$\lambda_{Me} = \begin{cases} \lambda(T), & T < T_{ev} \\ 10^{-2}\ W/m \cdot K, & T \geq T_{ev} \end{cases} \tag{7}$$

The latent heats of melting and evaporation are added to numerical model using the Irreversible Transformation option. This is also needed to escape a reverse transformation into a previous solid or liquid phase of demetallized area in case of cooling.

Adding the Electrical circuit module to the model allows simulating the MFC capacitance, its voltage and discharge during the simulated SH process.

III. EXPERIMENTAL RESULTS AND DISCUSSION

A. SMALL-SCALE INVESTIGATION RESULTS

The comparative analysis of the gate electrothermal destruction is shown in Figure 9.

The gate electrothermal destruction process results in the appearance of a narrow demetallized crack that electrically disconnects two neighboring segments. The photograph "Zinc3" in Fig. 9 shows incomplete destruction (in this case, the pulse width was shorter than τ_{dest}). As one can see, two demetallized cracks start propagating from both sides of the gate toward each other.

The specific action integral J was calculated basing on the experimental data (see example of current waveform in Fig.4). The experimental dependencies of specific action integral J on Al and Zn single gates destruction time τ_{dest} are presented in Fig. 10 (markers).

In the adiabatic approximation (the heat outflow is not taken into consideration) one can expect the constant level of deposited energy required for the electrothermal destruction of the gate. The corresponding J values for thin Al and Zn metals are about 1×10^{17} A^2s/m^4 and $(0.5-1)\times 10^{16}$ A^2s/m^4 respectively [17] and marked at the plot as dashed lines. However, one sees the significant growth of the specific action integral with the increase of destruction process duration due to the heat outflow to the polymer film. When the destruction time approaches zero value, the action integral becomes close to the value for adiabatic case.

The results obtained in small-scale experiments confirm the validity of the proposed model and the necessity of considering the heat outflow into the polymer layer when modelling.

B. LARGE-SCALE INVESTIGATION RESULTS

The results of the numerical simulation of electrothermal destruction in large-scale investigations are shown in Fig. 11. This image visualizes the formation of demetallized area in the intersegment gates and isolating of the segment. The image in Fig.11a corresponds to the moment of upper gates complete destruction and the partial destruction of lower ones. This nonsynchronous gates' destruction process is seen

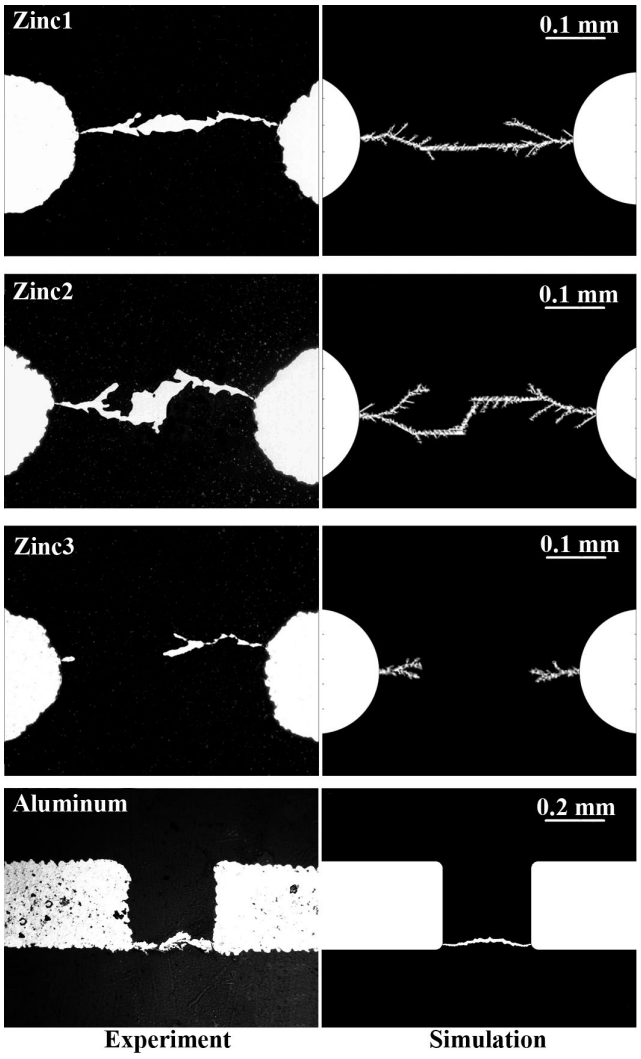

FIGURE 9. The examples of intersegments gates destruction in small-scale investigations.

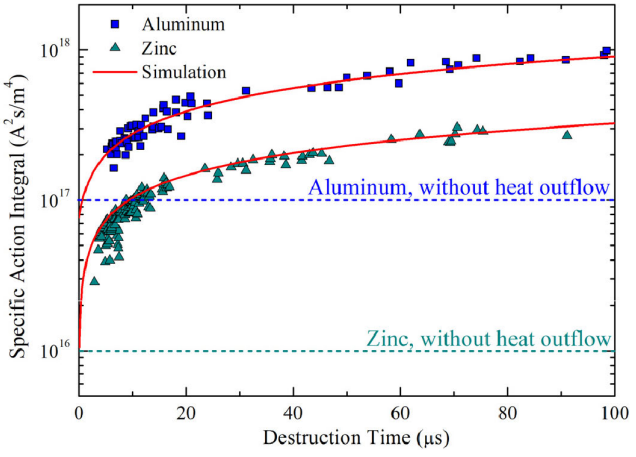

FIGURE 10. The specific action integral versus destruction time of Al and Zn gates.

in the current waveforms $I(t)$ (Fig. 11b). As a rule, experimental dependencies $I(t)$ have four falls that corresponds to each intersegment gate destruction. Since the simulation

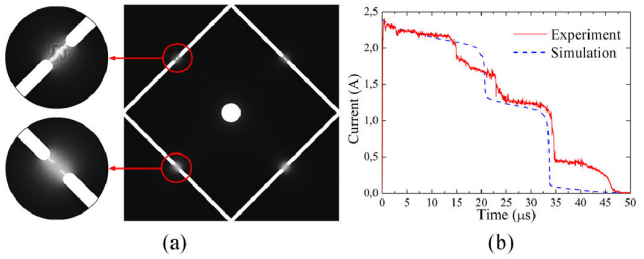

FIGURE 11. Numerical simulation of electrothermal destruction (a), and typical experimental and calculation current waveforms (b) in large-scale investigations.

model does not take into account irregularities of the metallization edges two upper gates and two lower ones are destructed in pairs respectively. Therefore, calculation current waveforms have only two falls. Nevertheless, the energy characteristics of the simulated and experimental processes are very close.

The video file with animated gates destruction and current waveform can be found in the supplementary files for this article. These results were used as the base for developing the complex simulation model for the MFC's designing.

IV. APPLICATION OF THE SIMULATION MODEL TO THE REAL CAPACITOR ELECTRODES DESIGN

The results of conducted experimental and theoretical investigations underlie the complex simulation model, which can be easily implemented as a software tool for the MFC's segmented electrodes design.

The model input data are:

- Nominal voltage;
- Capacitance;
- Thickness of the electrodes and polymer film;
- Thermal properties (density, specific heat capacity, thermal conductivity) of the electrodes metal and the polymer film;
- Electrical properties of the electrodes metal (resistivity, surface resistance);
- Geometric parameters of the segmented electrodes pattern;
- Ambient temperature.

The Tables 2 and 3 contain some simulation results, obtained by varying the following input parameters: b – the gate width, δ – the electrode thickness. In both cases the simulations were conducted for nominal voltage of capacitor $U_{nom} = 160$ V, intersegment distance 200 μm, segment side size 8 mm, ambient temperature 20 °C. R_s^* in the first column of the Table means the effective value of surface resistance of segmented electrodes. Because of the segmented pattern of the metallization the value R_s^* is higher than R_s of the all-over electrodes of the same thickness. The decrease in capacitance value $\Delta C/C_0$ (where C_0 is a capacitance for all-over metallization) caused by inactive intersegment gap is also presented in Table 2.

TABLE 2. Results of gate destruction simulation varying the gate width.

R_s*, Ω	$\Delta C/C$, %	b, μm	τ_{dest}, μs	J, $A^2 \cdot s/m^4$
Zinc, R_s=6 Ω, δ =20 nm				
24	4.84	200	2.85	9.1×10^{18}
22	4.81	250	4.25	1.0×10^{19}
21	4.78	300	6.00	2.0×10^{19}
20	4.75	350	8.80	2.2×10^{19}
19	4.72	400	11.5	2.4×10^{19}
19	4.69	450	15.0	4.3×10^{19}
18	4.66	500	19.5	4.6×10^{19}
Aluminum, R_s=3 Ω, δ =20 nm				
11.4	4.84	200	2.3	2.9×10^{18}
10.7	4.81	250	3.4	3.2×10^{18}
10.1	4.78	300	4.5	3.3×10^{18}
9.7	4.75	350	6.4	4.4×10^{18}
9.3	4.72	400	8.1	5.0×10^{18}
8.9	4.69	450	10.6	6.8×10^{18}
8.6	4.66	500	13.9	7.9×10^{18}

TABLE 3. Results of gate destruction simulation varying the electrode thickness.

R_s*, Ω	δ, nm	τ_{dest}, μs	J, $A^2 \cdot s/m^4$
Zinc, b =350 μm			
32	15	18.3	3.6×10^{19}
20	20	8.8	2.2×10^{19}
15	25	5.2	1.3×10^{19}
11	30	3.4	7.4×10^{18}
9	35	2.6	4.1×10^{18}
7	40	2.0	3.1×10^{18}
Aluminum, b =350 μm			
14.5	15	12.0	6.8×10^{18}
9.6	20	6.4	4.4×10^{18}
7.0	25	3.9	2.4×10^{18}
5.4	30	2.9	1.9×10^{18}
4.3	35	2.2	1.6×10^{18}
3.5	40	1.8	1.6×10^{18}

As can be seen, the model gives the opportunity to get the characteristics of developed segmented electrodes, such as single segment isolating time during SH, the energy required for the isolating, effective value of surface resistance R_s^*, that can be further used for the evaluation of MFC's ESR. The latter determines the performance of the MFC under high-current loads, which is limited by the losses in the electrodes rather than in low loss PP dielectric. The short segment isolating time leads to low SH energy value which diminishes the thermal impact on capacitor. On the one hand, it allows increasing the operating electric field in the dielectric and volumetric energy density. On the other hand, this reduces the thermal aging rate and the probability of thermal breakdown, thus improving the MFC reliability. The model can also be run in a parameter optimization mode when the electrode characteristics are estimated to meet the requirements for surface resistance, SH energy, SH duration, etc. The advantage of the simulation model is getting the optimal parameters of the segmentation pattern without conducting numerous experiments on different design samples, which implies the time and financial costs. The optimal parameters of the segmented electrodes ensure the timely initiation of SH process without the accidental gate destruction in high current operation. Thus, the application of the proposed model can help to increase the performance and reliability of the MFCs being developed.

V. CONCLUSION

One of the ways to increase the performance and operational reliability of metallized film capacitors is the segmented electrodes optimization. Considering the variety of possible electrodes patterns, the numerical simulation allows us to determine the optimal electrodes parameters, which give the highest value of electric field in the dielectric and the highest MFC reliability. In this paper, the results of experimental and numerical investigations of electrothermal destruction of the MFC segmented electrodes during the self-healing process were presented. The destruction processes were investigated for single gate and single segment, comprising four gates connected to the segment, cases. The experimental values of specific action integral J, which is proportional to the energy required for the gate destruction, the duration of destruction and other characteristics were obtained. For both cases the numerical models of gates electrothermal destruction were developed. It was shown that a significant part of the heat dissipated in the electrodes during the self-healing is absorbed by the polymer film. Based on experimental and theoretical background, the simulation model for the real MFC segmented electrodes design was developed. This model allows finding the optimal pattern of metallization for the given parameters. The advantage of the optimal pattern is increasing of the MFC's reliability and performance. Future work will be dedicated to the extension of the simulation model for such MFC's characteristics as: ESR, temperature and local overheating, ESL, etc.

ACKNOWLEDGMENT

The results of investigation were obtained using computational resources of Peter the Great St. Petersburg Polytechnic University Supercomputing Center (www.spbstu.ru).

REFERENCES

[1] N. Zhang, J. Ho, J. Runt, and S. Zhang, "Light weight high temperature polymer film capacitors with dielectric loss lower than polypropylene," *J. Mater. Sci., Mater. Electron.*, vol. 26, no. 12, pp. 9396–9401, Dec. 2015.

[2] J. Gao, D. K. Kwon, S. Perini, J. Long, S. Zhang, and M. T. Lanagan, "Glass dielectrics in extreme high-temperature environment," *J. Amer. Ceram. Soc.*, vol. 99, pp. 4045–4049, Dec. 2016.

[3] O. G. Gnonhoue, A. Velazquez-Salazar, É. David, and I. Preda, "Review of technologies and materials used in high-voltage film capacitors," *Polymers*, vol. 13, no. 5, p. 766, Feb. 2021.

[4] A. Yializis and Y. Ozaki, "Solid state polymer-multi-layer (PML) capacitors," in *Proc. 33rd Symp. Passive Electron. Compon.*, Houston, TX, USA, 2013, pp. 51–60.

[5] Q. Chen, Y. Shen, S. Zhang, and Q. M. Zhang, "Polymer-based dielectrics with high energy storage density," *Annu. Rev. Mater. Res.*, vol. 45, no. 1, pp. 433–458, Jul. 2015.

[6] J. R. MacDonald, M. A. Schneider, J. B. Ennis, F. W. MacDougall, and X. H. Yang, "High energy density capacitors," in *Proc. IEEE Electr. Insul. Conf.*, Montreal, QC, Canada, May 2009, pp. 306–309.

[7] R. M. Kerrigan and J. B. Ennis, "Pushing dielectrics to the limit—Self-healing metalized film capacitors for high energy density," in *Proc. IEEE 21st Int. Conf. Pulsed Power (PPC)*, Jun. 2017, pp. 1–4.
[8] M. Ritamaki, I. Rytoluoto, and K. Lahti, "Performance metrics for a modern BOPP capacitor film," *IEEE Trans. Dielectr. Electr. Insul.*, vol. 26, no. 4, pp. 1229–1237, Aug. 2019.
[9] V. O. Belko and O. A. Emelyanov, "Self-healing in segmented metallized film capacitors: Experimental and theoretical investigations for engineering design," *J. Appl. Phys.*, vol. 119, no. 2, Jan. 2016, Art. no. 024509.
[10] Y. Chen, H. Li, F. Lin, F. Lv, M. Zhang, Z. Li, and D. Liu, "Study on self-healing and lifetime characteristics of metallized-film capacitor under high electric field," *IEEE Trans. Plasma Sci.*, vol. 40, no. 8, pp. 2014–2019, Aug. 2012.
[11] M. Makdessi, A. Sari, and P. Venet, "Metallized polymer film capacitors ageing law based on capacitance degradation," *Microelectron. Rel.*, vol. 54, nos. 9–10, pp. 1823–1827, Sep. 2014.
[12] V. Belko, O. Emelyanov, and I. Ivanov, "Critical parameters of metallized film Capacitor's failure," in *Proc. IEEE 2nd Int. Conf. Dielectr. (ICD)*, Budapest, Hungary, Jul. 2018, pp. 1–3.
[13] V. Belko, I. Ivanov, A. Plotnikov, and V. Belanov, "Energy characteristics of self-healing process in metallized film capacitors," in *Proc. Int. Sci. Conf. Energy, Environ. Construct. Eng. (EECE)*, St. Petersburg, Russia, 2019, pp. 1–4.
[14] H. Li, H. Li, Z. Li, F. Lin, D. Liu, W. Wang, B. Wang, and Z. Xu, "T pattern fuse construction in segment metallized film capacitors based on self-healing characteristics," *Microelectron. Rel.*, vol. 55, no. 6, pp. 945–951, May 2015.
[15] H. Li, Z. Li, F. Lin, H. Jiang, T. Fang, and Q. Zhang, "Threshold current density of metallized film under multiple current pulses," *IEEE Trans. Plasma Sci.*, vol. 48, no. 7, pp. 2523–2530, Jul. 2020.
[16] S. Qin, S. Ma, and S. A. Boggs, "The mechanism of clearing in metalized film capacitors," in *Proc. IEEE Int. Symp. Electr. Insul.*, San Juan, PR, USA, Jun. 2012, pp. 592–595.
[17] O. A. Emelyanov and V. O. Belko, "Pattern formation in electrical exploding of thin metal films," *IEEE Trans. Plasma Sci.*, vol. 41, no. 4, pp. 961–966, Apr. 2013.

VICTOR O. BELKO (Member, IEEE) was born in Shevchenko, Russia. He received the B.Sc., Dipl.Ing., and Ph.D. degrees in electrical engineering from the Peter the Great St. Petersburg Polytechnic University, Saint Petersburg, Russia, in 2005, 2007, and 2010, respectively.

He is currently an Associate Professor with the Higher School of High-Voltage Engineering, Peter the Great St. Petersburg Polytechnic University. He has coauthored over 30 publications on power and pulse capacitors, dielectrics, and simulation. His current research interests include pulsed power, metal film capacitors, and electric explosion of conductors. He is a member of the IEEE Dielectrics and Electrical Insulation Society and the IEEE Nuclear and Plasma Sciences Society.

OLEG A. EMELYANOV (Senior Member, IEEE) was born in Leningrad, Russia, in 1961. He received the Dipl.Ing. degree in technical physics and the Ph.D. and Dr.Sci. degrees from the Peter the Great St. Petersburg Polytechnic University, Saint Petersburg, Russia, in 1984, 2004, and 2018, respectively. He is currently a Professor with the Peter the Great St. Petersburg Polytechnic University. He was a supervisor of six successful Ph.D. students and 22 M.Sc. students. His doctoral research focused on metal film capacitors in high overload modes. He has authored over 100 papers in scientific journals, technical reports, and conference proceedings. His current research interests include electrical capacitors, electrical discharges, cold atmospherics, and fast exploding wire plasmas. He is a member of the IEEE Dielectrics and Electrical Insulation Society and the IEEE Nuclear and Plasma Sciences Society.

IVAN O. IVANOV (Member, IEEE) received the B.Sc., M.Sc., and Ph.D. degrees in electrical engineering from the Peter the Great Saint-Petersburg Polytechnic University, Saint Petersburg, Russia, in 2010, 2012, and 2017, respectively. His first scientific experience was related to investigation of high-temperature superconductivity. From 2010 to 2012, he studied fast electromigration problem in thin metal layers. His Ph.D. dissertation was related to operating metallized film capacitors in overstressed modes, including high electric fields and high discharge currents. His current research interests include electrical capacitors, insulation of rotating machines, high voltage engineering, and numerical modeling.

ANDREY P. PLOTNIKOV (Member, IEEE) was born in Orenburg, Russia, in 1991. He received the B.Sc., M.Sc., and Ph.D. degrees in electrical engineering from the Peter the Great Saint-Petersburg Polytechnic University, Saint Petersburg, Russia, in 2012, 2014, and 2019, respectively.

Since 2015, he has been with the Peter the Great Saint-Petersburg Polytechnic University. He is currently an Assistant Professor with the Higher School of High-Voltage Engineering, Peter the Great St. Petersburg Polytechnic University. His current research interests include studying of ferroelectric capacitors performance under higher electro-thermal loads and dielectric loss of ferroelectric ceramics, self-healing processes in metal film capacitors characterization, and cold atmospheric electrical discharge plasmas.

EFREM G. FEKLISTOV (Graduate Student Member, IEEE) was born in Chelyabinsk, Russia, in 1994. He received the B.Sc. and M.Sc. degrees in electrical engineering from the Peter the Great Saint-Petersburg Polytechnic University, Saint Petersburg, Russia, in 2016 and 2018, respectively.

He is currently an Assistant Professor with the Higher School of High-Voltage Engineering, Peter the Great St. Petersburg Polytechnic University. His topical research interests include studying of cold atmospheric plasmas, partial discharges in metal film capacitors, and numerical modeling in high voltage engineering.